Inorganic Chemistry

Article

Self-Assembly, Reorganization, and Photophysical Properties of Silver(I)–Schiff-Base Molecular Rectangle and Polymeric Array Species

Huang-Chun Wu,[†] P. Thanasekaran,[†] Chi-Hwe Tsai,[†,‡] Jing-Yun Wu,[†] Sheng-Ming Huang,[†] Yuh-Sheng Wen,[†] and Kuang-Lieh Lu*,[†]

Institute of Chemistry, Academia Sinica, Taipei 115, Taiwan, and Department of Chemistry, National Central University, Chungli 320, Taiwan

A self-assembly of $AgClO_4$ with a Schiff-base ligand *N,N*′-bis(pyridin-2-ylmethylene)benzene-1,4-diamine (**1**) gave a 1D zigzag polymeric array $[\{Ag_2(C_{18}H_{14}N_4)_2\}(ClO_4)_2(CH_3CN)]_n$ (**3**), while the self-assembly of $AgClO_4$ with 3,3′-dimethyl-*N,N*′-bis(pyridin-2-ylmethylene)biphenyl-4,4′-diamine (**2**) afforded the molecular rectangle $[\{Ag_2(C_{26}H_{22}N_4)_2\}-(ClO_4)_2]$ (**4**). The structures of **3** and **4** were characterized by single-crystal X-ray diffraction analysis. Structural data for **3** indicate that the Ag(I) ion is coordinated by two ligands of **1** in a distorted tetrahedral fashion thereby leading to a 1D zigzag polymeric array. The zigzag chains are interdigitated with weak $\pi-\pi$ stacking interactions. The structure of **4** consists of a discrete molecular rectangle where the silver atom has a distorted square-planar coordination with the pyridyl ligands and azomethine nitrogen atoms of **2**. An intramolecular $\pi-\pi$ interaction between the phenyl rings of adjacent Schiff-base **2** functions to stabilize the rectangular architecture. The Ag(I)–Schiff-base coordination polymer **3** is not stable in solution. The degradation and reorganization of **3** to form a [2 × 2] grid architecture $[\{Ag_4(C_{26}H_{22}N_4)_4\}(ClO_4)_4]$ (**3g**) was supported in a FAB-MS study. The rectangular structure of **4** remains intact in solution at ambient temperature. The complexes **3g** and **4** exhibit unusual luminescence behavior in solution at room temperature with significantly red-shifted emission in the visible region.

Introduction

The design and self-assembly of functional materials has received considerable attention in recent years.[1–5] A combination of conjugated ligands and electron-rich metal centers can produce low-energy electronic interactions between metal centers and ligands, resulting in a product with interesting optical or electronic properties.[6] The Ag(I) ion is regarded as a soft acid that favors the coordination of soft bases, such as ligands that contain sulfur and unsaturated nitrogen.[7] Complexes of silver(I) and N-heterocyclic ligands lead to the production of interesting geometric configurations and

* To whom correspondence should be addressed. E-mail: lu@chem.sinica.edu.tw. Fax: Int. code + (2)27831237.

† Academia Sinica.

‡ National Central University.

(1) (a) Lehn, J. M. *Supramolecular Chemistry: Concepts and Perspectives*; VCH: Weinheim, Germany, 1995; Chapter 9. (b) Yaghi, O. M.; Li, G. *Angew. Chem., Int. Ed. Engl.* **1995**, *34*, 207–209. (c) Li, G. H.; Laine, A.; O'Keeffe, M.; Yaghi, O. M. *Science* **1999**, *283*, 1145–1147. (d) Li, H.; Eddaoudi, M.; O'Keeffe, M.; Yaghi, O. M. *Nature* **1999**, *402*, 276–279. (e) Kondo, M.; Shimamura, M.; Noro, S. i.; Minakoshi, S.; Asami, A.; Seki, K.; Kitagawa, S. *Chem. Mater.* **2000**, *12*, 1288–1299. (f) Schelter, E. J.; Bera, J. K.; Bacsa, J.; Galan-Mascaros, J. R.; Dunbar, K. R. *Inorg. Chem.* **2003**, *42*, 4256–4258. (g) Zhu, H. F.; Kong, L. Y.; Okamura, T. A.; Fan, J.; Sun, W. Y.; Ueyama, N. *Eur. J. Inorg. Chem.* **2004**, 1465–1473. (h) Kim, H. J.; Zin, W. C.; Lee, M. *J. Am. Chem. Soc.* **2004**, *126*, 7009–7014. (i) Ciurtin, D. M.; Pschirer, N. G.; Smith, M. D.; Bunz, U. H. F.; zur Loye, H. C. *Chem. Mater.* **2001**, *13*, 2743–2745. (j) Dong, Y. B.; Cheng, J. Y.; Huang, R. Q.; Smith, M. D.; zur Loye, H. C. *Inorg. Chem.* **2003**, *42*, 5699–5706.

(2) (a) Chambron, J. C.; Dietrich-Buchecker, C.; Sauvage, J. P. In *Comprehensive Supramolecular Chemistry*; Lehn, J. M., Atwood, J. L., Davies, J. E. D., MacNicol, D. D., Vogtle, F., Eds.; Pergamon: Oxford, U.K., 1996; Vol. 9, pp 43–83. (b) Lehn, J. M. *Chem.—Eur. J.* **2000**, *6*, 2097–2102. (c) Lehn, J. M. *Proc. Natl. Acad. Sci. U.S.A.* **2002**, *99*, 4763–4768. (d) Doumanidis, H. *Nanotechnology* **2002**, *13*, 248–252. (e) Banfi, S.; Carlucci, L.; Caruso, E.; Ciani, G.; Proserpio, D. M. *J. Chem. Soc., Dalton Trans.* **2002**, 2714–2721.

(3) (a) Desiraju, G. R. *Angew. Chem., Int. Ed. Engl.* **1995**, *34*, 2311–2327. (b) MacGillivray, L. R.; Atwood, J. L. *Nature* **1997**, *389*, 469–472. (c) Yaghi, O. M.; Li, G.; Li, H. *Nature* **1995**, *378*, 703–706. (d) Lehn, J. M. *Science* **2002**, *295*, 2400–2403. (e) Forster, S.; Plantenberg, T. *Angew. Chem., Int. Ed.* **2002**, *41*, 688–714. (f) Antonietti, M. *Nature Mater.* **2003**, *2*, 9–10. (g) Hamley, I. W. *Angew. Chem., Int. Ed.* **2003**, *42*, 1692–1712.

(4) (a) Yaghi, O. M.; Li, G. *Angew. Chem., Int. Ed. Engl.* **1995**, *34*, 207–209. (b) Leininger, B. Olenyuk, P. J. Stang, *Chem. Rev.* **2000**, *100*, 853–908. (c) Holliday, B. J.; Mirkin, C. A. *Angew. Chem., Int. Ed.* **2001**, *40*, 2022–2043. (d) Fujita, M. *Acc. Chem. Res.* **1999**, *32*, 53–61. (e) Swiegers, G. F.; Malefetse, T. J. *Chem. Rev.* **2000**, *100*, 3483–3538. (f) Seidel, S. R.; Stang, P. J. *Acc. Chem. Res.* **2002**, *35*, 972–983. (g) Schelter, E. J.; Bera, J. K.; Bacsa, J.; Galan-Mascaros, J. R.; Dunbar, K. R. *Inorg. Chem.* **2003**, *42*, 4256–4258.

Scheme 1. Preparation of Highly Conjugated Schiff Bases **1** and **2**
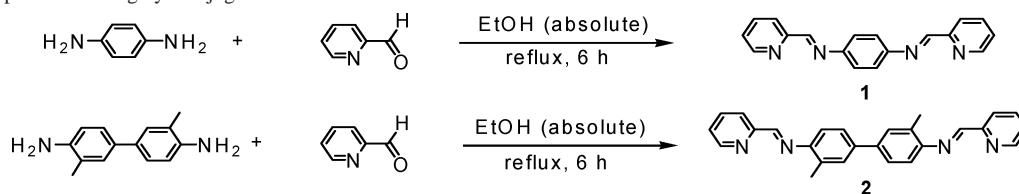
photophysical properties.[8−10] However, only a few examples of Ag(I)-containing Schiff-base complexes and coordination polymers have been studied in detail to date.[11] Recently, a luminescent Ag-based rectangle that assembled from silver nitrate and 1,3-bis(pyrrol-2-yl-methyleneamino)propane has been published.[12]

As part of our ongoing studies on the design and preparation of functional materials, we report herein on the self-assembly, reorganization, and photophysical properties of the Ag(I)−Schiff-base polymeric structure **3** and the discrete molecular rectangle **4**. The 1D zigzag compound **3** was observed to transform into a grid molecular topology in solution by a self-organization process whereas the rectangular complex **4** remains intact. These two Ag(I)−Schiff-base complexes exhibit luminescence behavior at room temperature. This is somewhat surprising, since other reported Ag(I)-based polymers show luminescence only in the solid state or at 77 K.[14−17]

Results and Discussion

Synthesis of Highly Conjugated Schiff Bases. The two highly conjugated Schiff-base ligands **1** and **2** were synthesized as yellow solids in high yields by the condensation of 2-pyridinecarboxaldehyde with 1,4-diaminobenzene and 3,3′-dimethylbenzidine, respectively (Scheme 1). Ligands **1** and **2** were characterized by spectroscopic methods. The ^{1}H NMR spectrum of **2** exhibited a singlet at δ 8.54 ppm, assigned to the resonance of the azomethine (CH=N) proton. The aromatic proton signals lie in the range δ 8.72−7.23 ppm while a singlet at δ 2.40 ppm indicates the presence of methyl groups.

The preparation of ligand **1** has been reported by Yoshida and co-workers,[18] whereas ligand **2** is a new compound. The main feature of these ligands is their exobidentate coordination mode via the pyridine and azomethine nitrogen atoms. The simplicity and high-yield synthesis, high conjugation, and versatile coordination capability make Schiff bases **1** and **2** interesting ligands for the study of self-assembly, self-organization with metal ions, and photophysical properties of their products.

Self-Assembly of Ag(I) Ion with the Schiff-Base Ligands. The self-assembly of **1** with AgClO$_4$ in a mixture of THF and CH$_3$CN at room temperature led to the formation of a coordination polymer [{Ag$_2$(C$_{18}$H$_{14}$N$_4$)$_2$}(ClO$_4$)$_2$·CH$_3$CN]$_n$

(5) (a) Hill, D. J.; Mio, M. J.; Prince, R. B.; Hughes, T. S.; Moore, J. S. *Chem. Rev.* **2001**, *101*, 3893−4012. (b) Yoshida, N.; Ichikawa, K. *Chem. Commun.* **1997**, 1091−1092. (c) Childs, L. J.; Pascu, M.; Clarke, A. J.; Alcock, N. W.; Hannon, M. J. *Chem.−Eur. J.* **2004**, *10*, 4291−4300. (d) Batten, S. R.; Robson, R. *Angew. Chem., Int. Ed.* **1998**, *37*, 1460−1494. (e) Kasai, K.; Aoyagi, M.; Fujita, M. *J. Am. Chem. Soc.* **2000**, *122,* 2140−2141.

(6) (a) Henary, M.; Wootton, J. L.; Khan, S. I.; Zink, J. I. *Inorg. Chem.* **1997**, *36*, 796−801. (b) Yam, V. W. W.; Lo, K. K. W. *J. Chem. Soc., Dalton Trans.* **1995**, 499−500. (c) Yam, V. W. W.; Lo, K. K. W. *Chem. Soc. Rev.* **1999**, *28*, 323−334.

(7) (a) Suenga, Y.; Kuroda-Sowa, T.; Maekawa, M.; Munakata, M. *J. Chem. Soc., Dalton Trans*. **2000**, 3620−3623. (b) Hannon, M. J.; Painting, C. L.; Alcock, N. W. *Chem. Commun.* **1999**, 2023−2024. (c) Bu, X. H.; Chen, W.; Hou, W. F.; Du, M.; Zhang, R. H.; Brisse, F. *Inorg. Chem.* **2002**, *41*, 3477−3482. (d) Ouyang, X. M.; Fei, B. L.; Okamura, T. A.; Bu, H. W.; Sun, W. Y.; Tang, W. X.; Ueyama, N. *Eur. J. Inorg. Chem.* **2003**, 618−627. (e) Blake, A. J.; Gould, R. O.; Li, W. S.; Lippolis, V.; Parsons, S.; Radek, C.; Schroder, M. *Inorg. Chem.* **1998**, *37*, 5070−5077. (f) Blower, P. J.; Clarkson, J. A.; Rawle, S. C.; Hartman, J. A. R.; Wolf, R. E., Jr.; Yagbasan, R.; Bott, S. G.; Cooper, S. R. *Inorg. Chem.* **1989**, *28*, 4040−4046.

(8) (a) Catalano, V. J.; Kar, H. M.; Garnas, J. *Angew. Chem., Int. Ed.* **1999**, *38*, 1979−1982. (b) Zhang, G. q.; Yang, G. q.; Yang, L. y.; Chen, Q. q.; Ma, J. S. *Eur. J. Inorg. Chem.* **2005**, 1919−1926. (c) Huang, X. C.; Zheng, S. L.; Zhang, J. P.; Chen, X. M. *Eur. J. Inorg. Chem.* **2004**, *5*, 1024−1029. (d) Ren, C. X.; Ye, B. H.; He, F.; Cheng, L.; Chen, X. M. *CrystEngCommun* **2004**, *6*, 200−206.

(9) (a) Dong, Y.-B.; Cheng, J.-Y.; Ma, J.-P.; Huang, R.-Q.; Smith, M. D. *Cryst. Growth Des.* **2005**, *5*, 585−591. (b) Catalano, V. J.; Malwitz, M. A. *Inorg. Chem.* **2003**, *42*, 5483−5485. (c) Kang, Y.; Seward, C.; Song, D.; Wang, S. *Inorg. Chem.* **2003**, *42*, 2789−2797. (d) Ouyang, X. M.; Liu, D. J.; Okamura, T. a.; Bu, H. W.; Sun, W. Y.; Tang, W. X.; Ueyama, N. *Dalton Trans.* **2003**, 1836−1845. (e) Yam, V. W. W.; Lo, W. Y.; Zhu, N. *Chem. Commun.* **2003**, 2446−2447.

(10) (a) Munakata, M.; Wu, L. P.; Kuroda-Sowa, T.; Maekawa, M.; Suenaga, Y.; Ning, G. L.; Kojima, T. *J. Am. Chem. Soc.* **1998**, *120,* 8610−8618. (b) Schmidbaur, H.; Bublak, W.; Huber, B.; Reber, G.; Muller, G. *Angew. Chem., Int. Ed. Engl.* **1986**, *25*, 1089−1090. (c) Che, C. M.; Yip, H. K.; Li, D.; Peng, S. M.; Lee, G. H.; Wang, Y. M.; Liu, S. T. *J. Chem. Soc., Chem. Commun.* **1991**, 1615−1617. (d) Wu, C. D.; Ngo, H. L.; Lin, W. *Chem. Commun.* **2004**, 1588−1589.

(11) (a) Liu, M.; Xu, G.; Liu, Y.; Chen, Q. *Langmuir* **2001**, *17*, 427−431. (b) Chen-jie, F.; Chun-ying, D.; Hong, M.; Cheng, H.; Qing-jin, M.; Yong-jiang, L.; Yu-hua, M.; Zhe-ming, W. *Organometallics* **2001**, *20*, 2525−2532. (c) Patra, G. K.; Goldberg, I. *Cryst. Growth Des.* **2003**, *3*, 321−329. (d) Hou, H.; Li, G.; Song, Y.; Fan, Y.; Zhu, Y.; Zhu, L. *Eur. J. Inorg. Chem.* **2003**, 2325−2332. (e) Dong, Y. B.; Zhao, X.; Huang, R. Q.; Smith, M. D.; zur Loye, H. C. *Inorg. Chem.* **2004**, *43*, 5603−5612. (f) Dong, Y. B.; Zhao, X.; Tang, B.; Wang, H. Y.; Huang, R. Q.; Smith, M. D.; zur Loye, H. C. *Chem. Commun.* **2004**, 220−221.

(12) Zhang, G.; Yang, G.; Ma, J. S. *Inorg. Chem. Commun.* **2004**, *7*, 994−997.

(13) (a) Liu, Y. H.; Lu, Y. L.; Wu, H. C.; Wang, J. C.; Lu, K. L. *Inorg. Chem.* **2002**, *41*, 2592−2597. (b) Liu, Y. H.; Tsai, H. L.; Lu, Y. L.; Wen, Y. S.; Wang, J. C.; Lu, K. L. *Inorg. Chem.* **2001**, *40*, 6426−6431. (c) Luo, T. T.; Liu, Y. H.; Tsai, H. L.; Su, C. C.; Ueng, C. H.; Lu, K. L. *Eur. J. Inorg. Chem.* **2004**, 4253−4258.

(14) (a) Blake, A. J.; Champness, N. R.; Hubberstey, P.; Li, W. S.; Withersby, M. A.; Schroder, M. *Coord. Chem. Rev.* **1999**, *183*, 117−138. (b) Dong, Y. B.; Jin, G. X.; Smith, M. D.; Huang, R. Q.; Tang, B.; zur Loye, H. C. *Inorg. Chem.* **2002**, *41*, 4909−4914. (c) Baxter, P. N. W. *J. Org. Chem.* **2004**, *69,* 1813−1821. (d) Seward, C.; Chan, J.; Song, D.; Wang, S. *Inorg. Chem.* **2003**, *42,* 1112−1120.

(15) (a) Catalano, V. J.; Malwitz, M. A.; Etogo, A. O. *Inorg. Chem.* **2004**, *43,* 5714−5724. (b) Bu, X. H.; Xie, Y. B.; Li, J. R.; Zhang, R. H. *Inorg. Chem.* **2003**, *42,* 7422−7430.

(16) (a) Ouyang, X. M.; Fei, B. L.; Okamura, T. a.; Bu, H. W.; Sun, W. Y.; Tang, W. X.; Ueyama, N. *Eur. J. Inorg. Chem.* **2003**, 618−627. (b) Pascu, M.; Tuna, F.; Kolodziejczyk, E.; Pascu, G. I.; Clarkson, G.; Hannon, M. J. *Dalton Trans.* **2004**, 1546−1555. (c) Hamblin, J.; Jackson, A.; Alcock N. W.; Hannon, M. J. *J. Chem. Soc., Dalton Trans.* **2002**, 1635−1641.

(17) Tuna, F.; Clarkson, G.; Alcock, N. W.; Hannon, M. J. *Dalton Trans.* **2003**, 2149−2155.

(18) Yoshida, N.; Ichikawa, K.; Shiro, M. *J. Chem. Soc., Perkin Trans. 2* **2000**, 17−26.

Scheme 2. Self-Assembly of Ag(I)−Schiff-Base Compounds **3** and **4** at Room Temperature

AgClO$_4$ + [structure **1**] $\xrightarrow[\text{30 °C}]{\text{THF/CH}_3\text{CN}}$ [{Ag$_2$(C$_{18}$H$_{14}$N$_4$)$_2$}(ClO$_4$)$_2$(CH$_3$CN)]$_n$

1 **3**

AgClO$_4$ + [structure **2**] $\xrightarrow[\text{30 °C}]{\text{THF/MeOH/C}_6\text{H}_5\text{NO}_2}$ [{Ag$_2$(C$_{26}$H$_{22}$N$_4$)$_2$}(ClO$_4$)$_2$]

2 **4**
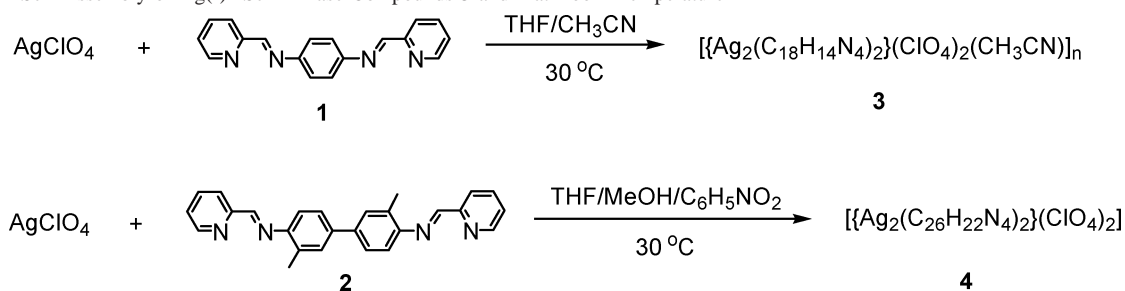
(**3**) with a 1D zigzag structure in high yield. The slow diffusion of a solution of **2** in nitrobenzene into a solution of AgClO$_4$ in a mixture of toluene/MeOH afforded the orange-colored crystalline rectangle [{Ag$_2$(C$_{26}$H$_{22}$N$_4$)$_2$}-(ClO$_4$)$_2$] (**4**) (Scheme 2). Compounds **3** and **4** were characterized by spectral methods, and their structures were further confirmed by single-crystal X-ray diffraction analyses. The ^{1}H NMR spectra of **3** and **4** showed that both pyridyl and azomethine (C*H*=N) proton signals are shifted downfield relative to those of the free ligands, indicating the coordination of the Schiff bases with Ag(I) ions. For compound **4**, one singlet appeared at δ 8.75 ppm assigned to an imine (C*H*=N) proton. The presence of one singlet at δ 2.17 ppm corresponds to methyl groups. Compounds **3** and **4** are soluble in highly polar solvents such as CH$_3$CN, DMSO, DMF, THF, MeOH, and EtOH.

Crystal Structure of 3. A single-crystal diffraction analysis of **3** revealed that the Ag(I) ion is coordinated by two Schiff bases via pyridyl and azomethine nitrogen atoms. One Schiff base is coordinated to two Ag(I) atoms. A distorted tetrahedral configuration is observed around the metal center thereby generating a 1D zigzag coordination polymer. An ORTEP diagram of **3** is shown in Figure 1,
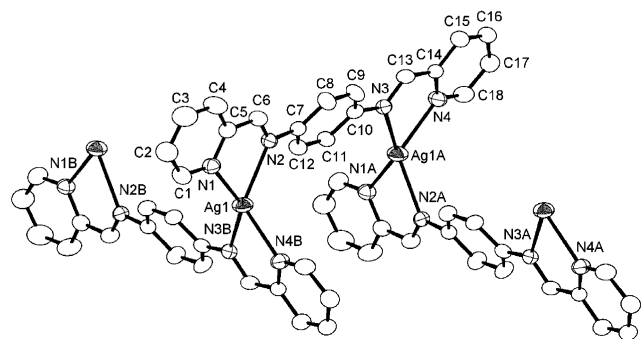
Figure 1. Local coordination environment of Ag(I) in **3**. Atoms are represented as 30% thermal ellipsoids. All anions are omitted for clarity.

and pertinent crystallographic data are given in Tables 1 and 2. The Ag−N$_{pyridyl}$ bond lengths are in the range 2.290(5)−2.356(5) Å, while the Ag−N$_{azomethine}$ bond distances lie in the range 2.303(5)−2.395(4) Å. All these bond lengths are consistent with those reported for other Ag−Schiff-base complexes.[10] The bond angles of N(1)−Ag(1)−N(2) and N(3)−Ag(1A)−N(4) are 72.2(2) and 71.8(2)°, respectively. The packing diagram shows that the zigzag chains are interdigitated with $\pi-\pi$ stacking with a distance of ca. 3.6 Å between the Schiff-base ligands (Figure 2). Janiak reported

Table 1. Crystal Structure Refinement Data for **3** and **4**

param	3	4
empirical formula	C$_{38}$H$_{31}$Ag$_2$Cl$_2$N$_9$O$_8$	C$_{52}$H$_{48}$Ag$_2$Cl$_{1.5}$N$_8$O$_8$
fw	1028.36	1184.90
cryst system	monoclinic	monoclinic
space group	C2/c	C2/c
a, Å	28.7440(18)	13.4902(4)
b, Å	10.2680(8)	27.4260(10)
c, Å	14.7940(12)	29.1409(10)
β, deg	113.535(5)	102.258(2)
V, Å^3	4003.1(5)	10535.8(6)
Z	4	8
T, K	298	273(2)
diffractometer	Kappa CCD	SMART CCD
λ, Å	0.710 73	0.710 73
D$_{calcd}$, g/cm^3	1.706	1.494
μ, mm^{-1}	1.176	0.880
F(000)	2056	4808
θ, deg	2.13−25.10	1.43−25.06
reflcns measd	11 908	50 840
indep reflcns	3513 (R$_{int}$ = 0.0648)	9239 (R$_{int}$ = 0.2540)
reflcns obsd [I > 2σ(I)]	2090	1629
params	268	642
R1^a [I > 2σ(I)]	0.0559	0.0691
wR2^a [I > 2σ(I)]	0.1338	0.1811
R1 (all data)	0.1130	0.3308
wR2 (all data)	0.1657	0.2130
goodness-of-fit	1.065	0.663
$\Delta\rho_{max}/\Delta\rho_{min}$ (e Å^{-3})	0.579/−0.492	1.174/−0.443

^{a} R1 = $\Sigma||F_o| - |F_c||/\Sigma|F_o|$, wR2 = $[\Sigma w(F_o^2 - F_c^2)^2/\Sigma w(F_o^2)^2]^{1/2}$.

Table 2. Selected Bond Lengths (Å) and Angles (deg) for **3** and **4**^{a}

Compound 3			
Ag(1)−N(1)	2.290(5)	Ag(1)−N(2)	2.396(4)
Ag(1)−N(3)#1	2.304(5)	Ag(1)−N(4)#1	2.356(5)
N(2)−C(6)	1.265(8)	N(3)−C(13)	1.279(7)
N(1)−Ag(1)−N(3)#1	140.72(18)	N(1)−Ag(1)−N(4)#1	126.54(18)
N(3)#1−Ag(1)−N(4)#1	71.84(18)	N(1)−Ag(1)−N(2)	72.19(18)
N(3)#1−Ag(1)−N(2)	130.37(17)	N(4)#1−Ag(1)−N(2)	124.35(17)

Compound 4			
Ag(1)−N(1)	2.200(18)	Ag(1)−N(2)	2.422(16)
Ag(1)−N(101)	2.409(18)	Ag(1)−N(102)	2.289(13)
Ag(1)−N(201)	2.226(17)	Ag(1)−N(202)	2.343(14)
Ag(1)−N(301)	2.289(13)	Ag(1)−N(302)	2.534(13)
N(2)−C(6)	1.213(18)	N(102)−C(106)	1.319(16)
N(202)−C(206)	1.246(17)	N(302)−C(306)	1.304(17)
N(1)−Ag(1)−N(2)	73.0(6)	N(1)−Ag(1)−N(201)	121.5(7)
N(1)−Ag(1)−N(202)	160.0(6)	N(2)−Ag(1)−N(201)	155.8(5)
N(2)−Ag(1)−N(202)	101.2(6)	N(201)−Ag(1)−N(202)	71.3(6)
N(101)−Ag(2)−N(102)	70.4(6)	N(101)−Ag(2)−N(301)	108.7(7)
N(101)−Ag(2)−N(302)	167.2(5)	N(102)−Ag(2)−N(301)	170.9(4)
N(102)−Ag(2)−N(302)	110.3(6)	N(301)−Ag(2)−N(302)	72.7(6)

^{a} Symmetry transformations used to generate equivalent atoms: for **3**, (#1) −x + 1/2, y + 1/2, −z + 1/2; for **4**, (#1) −x + 1, y, −z + 1/2.

that strong $\pi-\pi$ stacking interactions are operative in metal complexes with aromatic ligands when the plane-to-plane distances are around 3.3 Å.[19] The $\pi-\pi$ interactions in **3** are comparatively weak since 3.6 Å is near the maximum (3.8
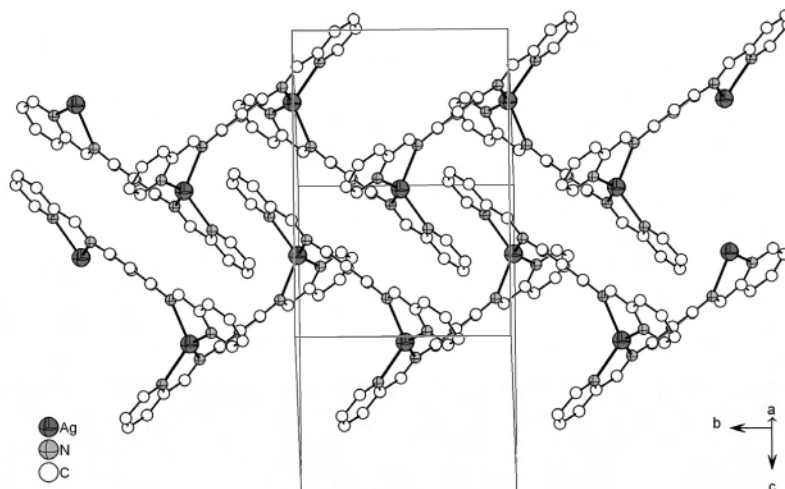
Figure 2. Crystal packing diagram of **3** showing the $\pi-\pi$ stacking between zigzag chains. Perchlorate ions and acetonitrile molecules are omitted for clarity.
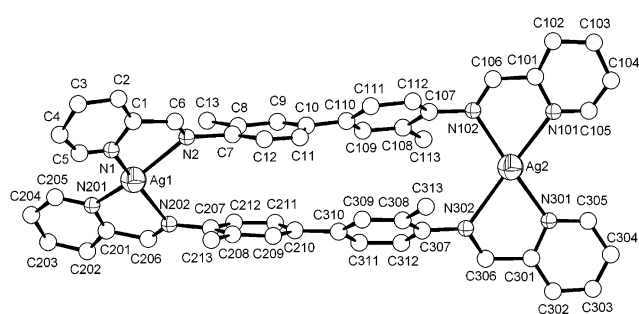
Figure 3. Molecular rectangle framework of cationic $[Ag_2(\mathbf{2})_2]^{2+}$ in **4**, showing the coordination environment around the Ag ions.

Å) for which $\pi-\pi$ interactions are accepted.[19] The perchlorate ions do not coordinate to the Ag(I) ions but are located between the layers.

Crystal Structure of 4. Crystals of $[\{Ag_2(C_{26}H_{22}N_4)_2\}$-$(ClO_4)_{1.5}(OH)_{0.5}]\cdot0.25CH_3OH\cdot1.25H_2O$ (**4**), suitable for single-crystal X-ray diffraction analysis, were obtained from the self-assembly of $AgClO_4$ with ligand **2** in a mixture of nitrobenzene, toluene, and MeOH at ambient temperature. The resolved solid-state structure reveals that **4** is consistent with a molecular rectangle. An ORTEP diagram of **4** is shown in Figure 3, and pertinent crystallographic data are given in Tables 1 and 2. The cationic molecular rectangle in **4** consists of two Ag(I) and two Schiff-base ligands **2**. Each Schiff base is doubly chelated and bridges two silver atoms while each Ag(I) is coordinated to two pyridyl and two azomethine nitrogen atoms, generating a four-coordinated distorted square-planar geometry. The Ag$-$N$_{pyridyl}$ bond lengths are in the range 2.200(18)$-$2.409(18) Å, while the Ag$-$N$_{azomethine}$ bond distances lie in the range 2.289(13)$-$2.534(13) Å (Table 2). The bite angles of N$_{pyridyl}-$Ag$-$N$_{azomethine}$ are in the range 70.4(6)$-$73.0(6)°. The four aromatic rings of the Schiff-base ligand **2** in the structure of **4** are not coplanar, with dihedral angles of 50.94$-$63.70° between the iminopyridine planes and the linked phenyl rings and dihedral angles of 29.68$-$33.67° between the two central phenyl rings. Intramolecular $\pi-\pi$ interactions between the

phenyl rings of the Schiff-base **2** with centroid···centroid distances of 3.66 and 3.89 Å stabilize the rectangular architecture of **4** (Figure 3). One and a half perchlorates together with half of a hydroxyl ion have been characterized in compensating the charge induced by silver ions. The reason for obtaining such a mixed-anion species is not clear. When viewed along the crystallographic b-axis, six arene columns fabricated by alternative intra- (3.66 Å) and intermolecular $\pi-\pi$ (3.77 and 3.92 Å) interactions are observed (Figure 4). If ligand **2** reacted with Ag(I) to form a similar 1D zigzag chain as **3**, the intermolecular $\pi-\pi$ interactions would be very weak or even impossible, as the spacer of two conjugated benzene rings is too long to form an interdigitated structure. However, the intramolecular $\pi-\pi$ interaction of the arene rings in complex **4** appear to be significant to stabilize the rectangular structure, although it is not strong. It can be reasonably assumed that the spacers between the two iminopyridine groups in **1** and **2** would effectively tune the self-assembly pathways, giving rise to different products, a 1D zigzag chain **3** and a molecular rectangle **4**.

Reorganization of 3 in Solution. It is noteworthy that some silver(I) entities are labile in solution at room temperature.[20] Compounds **3** and **4** adopt different molecular topologies in the solid state consisting of highly conjugated Schiff bases with silver ions. It is thus of particular interest to examine the solution behaviors of **3** and **4**. FAB-MS spectrometry has been found to be particularly useful for the identification of large metallosupramolecular architectures in solution.[21] As a consequence, a FAB-MS analysis of **3** and **4** in acetonitrile solution was performed to gain further information concerning the structures of **3** and **4** in solution. The FAB-MS spectrum of **3** exhibited a molecular ion peak

(19) Janiak, C. *J. Chem. Soc., Dalton Trans.* **2000**, 3885$-$3896.

(20) (a) Provent, C.; Rivara-Minten, E.; Hewage, S.; Brunner, G.; Williams, A. F. *Chem.—Eur. J.* **1999**, *5*, 3487$-$3494. (b) Khlobystov, A.; Blake, A. J.; Champness, N. R.; Lemenovskii, D. A.; Majouga, A. G.; Zyk, N. V.; Schroder, M. *Coord. Chem. Rev.* **2001**, *222*, 155$-$192.

(21) (a) Woessner, S. M.; Helms, J. B.; Houlis, J. F.; Sullivan, B. P. *Inorg. Chem.* **1999**, *38*, 4380$-$4381. (b) Johnston, M. R.; Latter, M. J.; Warrener, R. N. *Org. Lett.* **2002**, *4*, 2165$-$2168. (c) ALQaisi, S. M.; Galat, K. J.; Chai, M.; Ray, D. G., III; Rinaldi, P. L.; Tessier, C. A.; Youngs, W. J. *J. Am. Chem. Soc.* **1998**, *120*, 12149$-$12150.

Figure 4. Perspective view of the six-arene columns (gray arenes) architecture built from the inter- and intramolecular $\pi-\pi$ interactions in **4**.
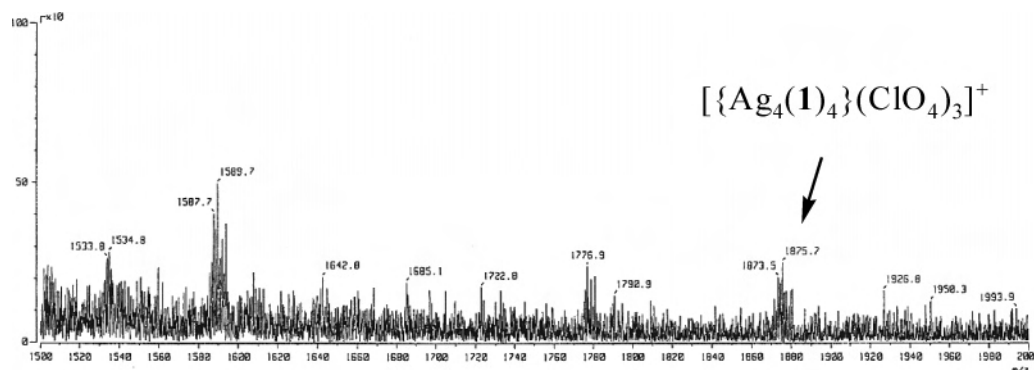
Figure 5. FAB-MS spectrum of **3** in CH_3CN solution.

Scheme 3. Reorganization of Complex **3** in Solution State

$[\{Ag_2(\mathbf{1})_2\}(ClO_4)_2(CH_3CN)]_n$ $\xrightarrow[\text{reorganization}]{CH_3CN}$ $[\{Ag_4(\mathbf{1})_4\}(ClO_4)_4]$

1D zigzag chain   grid

3 (solid state)   **3g** (solution state)

$[\{Ag_2(\mathbf{2})_2\}(ClO_4)_2]$ $\xrightarrow{CH_3CN}$ $[\{Ag_2(\mathbf{2})_2\}(ClO_4)]$

rectangle   rectangle

4 (solid state)   **4** (solution state)
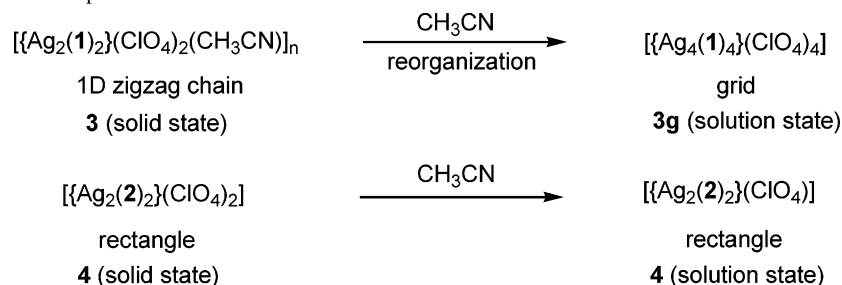
at $m/z = 1875.7$ corresponding to a grid species $[\{Ag_4(\mathbf{1})_4\}-(ClO_4)_3]^+$ (Figure 5).

This MS data supported the presence of a grid species $[\{Ag_4(\mathbf{1})_4\}(ClO_4)_4]$ (**3g**) in solution when **3** dissolved in CH_3CN. This is corroborated by the symmetrical pattern of the proton signals in the ^1H NMR spectrum of **3g**, which showed an azomethine (CH=N) proton signal at δ 8.87 ppm, a phenyl proton singal at δ 7.37 ppm, and pyridyl proton signals at δ 8.89 (H^6), 8.17 (H^4), 8.10 (H^3), and 7.75 (H^5) ppm. The generation of **3g** is probably due to the fragmentation of polymer **3** and reorganization of a tetranuclear grid during the dissolution process.[22] von Zelewsky and coworkers recently reported that a polymeric double-helix complex breaks down in solution to produce circular helicates or oligomers which are in rapid dynamic equilibrium.[23] It is noteworthy in this respect that a small difference in poly-

nucleating ligands can determine a gridlike or a helicate structure while the metal ion coordinates with polypyridyl ligands.[24] It has been shown that 3,6-bis(2-pyridyl)pyridazine can act as a metal-coordinating ligand for silver ion, resulting in the production of gridlike metal complexes.[25] On the basis of these observations, we assume that $[\{Ag_4(\mathbf{1})_4\}(ClO_4)_4]$ (**3g**) is most likely to possess a [2 × 2] gridlike structure in solution (Scheme 3 and Figure 6).

The FAB-MS analysis of **4** exhibits a signal corresponding to the $[\{Ag_2(\mathbf{2})_2\}(ClO_4)]^+$ ion at $m/z = 1096.9$, suggesting

(22) Mimassi, L.; Guyard-Duhayon, C.; Raehm, L.; Amouri, H. *Eur. J. Inorg. Chem.* **2002**, 2453−2457.

(23) Mamula, O.; von Zelewsky, A.; Bark, T.; Bernardinelli, G. *Angew. Chem., Int. Ed.* **1999**, *38*, 2945−2948.

(24) (a) Rojo, J.; Romero-Salguero, F. J.; Lehn, J. M.; Baum, G.; Fenske, D. *Eur. J. Inorg. Chem.* **1999**, 1421−1428. (b) Constable, E. C.; Chotalia, R. *J. Chem. Soc., Chem. Commun.* **1992**, 64−66.

(25) (a) Baxter, P. N. W.; Lehn, J. M.; Kneisel, B. O.; Fenske, D. *Angew. Chem., Int. Ed. Engl.* **1997**, *36*, 1978−1981. (b) Weissbuch, I.; Baxter, P. N. W.; Kuzmenko, I.; Cohen, H.; Cohen, S.; Kjaer, K.; Howes, P. B.; Als-Nielsen, J.; Lehn, J. M.; Leiserowitz, L. Lahav, M. *Chem.−Eur. J.* **2000**, *6*, 725−734.
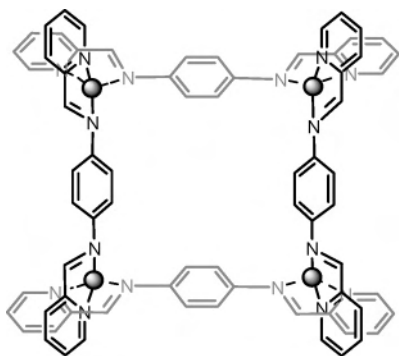
Figure 6. [2 × 2] grid-type structure of **3g** in solution.

that the rectangular structure of **4** in solution remains intact (Figure 7). This result is corroborated by the ^{1}H NMR data for **4**, which shows the presence of a highly symmetrical species.

Interestingly, the reorganization of the coordination polymer **3** proceeds spontaneously to form the grid species **3g** in solution while the molecular rectangle **4** retains the same structure in both the solid and solution states. Owing to the labile nature of the bonding between Ag(I) ion and Schiff-base **1**, the 1D chain structure **3** degrades in solution, and then the components undergo self-organization to form the tetranuclear grid **3g**, whereas the rectangular structure **4** formed from **2** and Ag(I) ion contains intramolecular $\pi-\pi$ interactions which probably contributes to the stability of the rectangle both in solution and solid states (Scheme 4).

Photophysical Properties. The electronic absorption spectra of **3g** and **4** in CH$_3$CN solution display intense absorption bands associated with intraligand (IL) and metal-perturbed intraligand transitions (MPIL) in the range 200−361 nm (Figures 8 and 9). These complexes may have a slight metal-to-ligand charge transfer (MLCT) characteristic

at 353 nm for **3g** and 363 nm for **4**.[26] The luminescent properties of **3** (**3g** in solution) and **4** were investigated in the solid state and in CH$_3$CN solution, and their absorption and emission maxima are compiled in Table 3. It has been shown that the chemical nature, the size, and the position of the substituents in the ligand can affect the geometry of the excited state, which influences the emission properties.[27,28] Ligands **1** and **2** display a very weak luminescence at 400−521 nm in solution (λ_{ex} = 355 and 362 nm for **1** and **2**, respectively) at room temperature while strong luminescence is observed at 457 and 527 (sh) nm for **3g** and 409, 432 (sh), 505, and 526 (sh) nm for **4** upon irradiation at 353 and 363 nm, respectively (Figures 8 and 9). The enormous enhancement in luminescence in **3g** and **4** can be attributed to the chelation of the ligand to the Ag center, which increases the conformational rigidity of the ligands. This leads to reduce the nonradiative decay of the intraligand $^1\pi-\pi^*$ excited state. In addition, in view of the emission lifetimes of complexes **3g** and **4** in solution at 298 K, it is likely that the excited states of **3g** and **4** are mixed with a $^3\pi-\pi^*$ character. Biexponential decays are observed for both **3g** and **4**, and the short- and long-lived components are assigned to ligand-based as well as metal-perturbed intraligand transitions. One possible explanation for the higher lifetime of **4** than **3g** is the extended π-conjugation of **2**. Furthermore, an intramolecular $\pi-\pi$ interaction also leads to a significant enhancement in the lifetime of **4**. The sensitivity of luminescence of **2** toward Ag(I) ion and intramolecular $\pi-\pi$ interaction makes it potentially useful as a fluorescent sensor for certain metal ions and molecules. In general, Ag(I) complexes might emit a weak photoluminescence at low temperature. Surprisingly, complexes **3**, **3g**, and **4** represent unusual examples of room-temperature luminescent Ag-containing compounds.[29] Note that the emission and absorp-

$$[\{Ag_2(\mathbf{2})_2\}(ClO_4)]^+$$
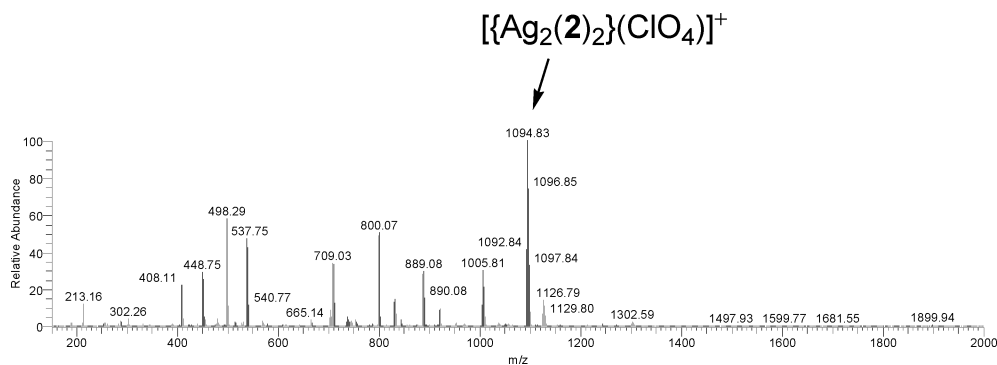
Figure 7. FAB-MS spectrum of **4** in solution.

Scheme 4. Self-Assembly and Self-Organization of 1D Chain **3**, [2 × 2] Gridlike Structure **3g**, and Rectangular Complex **4** from Silver Ion and Schiff-Base Ligands **1** and **2**
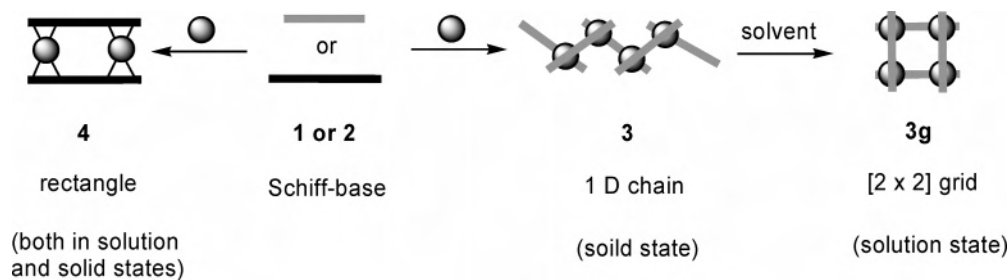
Table 3. Photophysical Data for **1−4** in CH$_3$CN at Room Temperature

compd	λ_{max}^{abs}, nm	λ_{max}^{em}, nm	τ, ns	λ_{max}^{em}, nm[a]
1	204, 237, 286, 355	411, 432	nd	
2	208, 241, 284, 362	451, 521	nd	
3[b]	204, 237, 286, 353	457, 527 (sh)	1.3,[c] 1.2[d]	471, 537, 630
4	206, 242, 282, 363	409, 432 (sh), 505, 526 (sh)	12.7,[e] 1.79[f]	560

[a] λ_{ex} = 360 nm in the solid state for **3** and **4**. [b] 1D polymer in solid state; [2 × 2] grid in solution state. [c] λ_{em} = 457 nm. [d] λ_{em} = 527 nm. [e] λ_{em} = 409 nm. [f] λ_{em} = 505 nm; nd = not detectable.
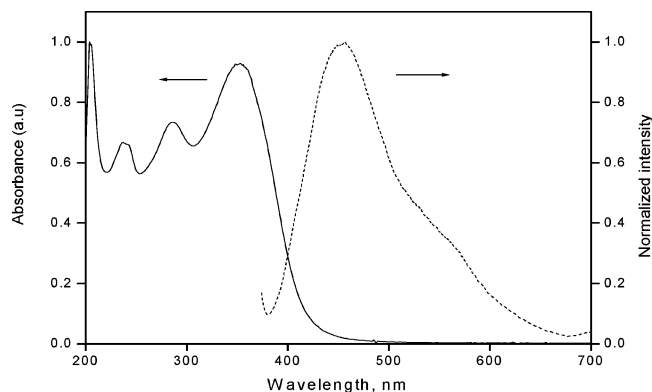
Figure 8. Absorption and emission spectra of **3g** in CH$_3$CN at room temperature.
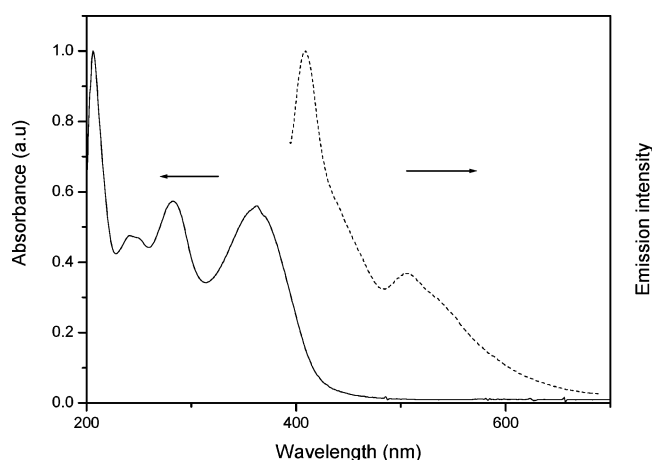
Figure 9. Absorption and emission spectra of molecular rectangle **4** in CH$_3$CN at room temperature.

tion maxima of metal-perturbed intraligand transitions (MPIL) for complex **4** are in the lower energy region with a higher lifetime than those of **3g** due to the effect of extended π-conjugation.

In the solid state, broad, structureless emission spectra with maxima at 471, 537, and 630 nm for **3** and 560 nm for **4** were observed. The origin of the emission band at 537 nm for **3** and 560 nm for **4** is believed to be the result of metal-perturbed IL transitions, whereas the high-energy emission at 400−460 nm is mainly associated with IL π−π* transitions. The emission observed at 630 nm for **3** may be due to

a metal-to-ligand charge-transfer transition whereas **4** does not emit luminescence in this region because of the dominating intramolecular π−π interactions of **2**, i.e., mixing of the ^{3}π−π* character of **2**. It is important to mention that only a few Ag(I)-containing coordination polymers exhibit such a type of characteristic emission above 600 nm in the solid state.[14b,c,26,30]

Redox Properties. To provide further evidence for the assignment of **3g** and **4**, their redox behaviors were examined by both cyclic and differential pulse voltammetric techniques. Complex **3g** displays an irreversible reduction wave at −0.25 V (versus Ag/Ag$^+$), corresponding to Ag(I) metal-centered reduction. On the other hand, the quasireversible reduction at −1.46 and −1.91 V (versus Ag/Ag$^+$) in **3g** corresponds to a pyridyl ligand-centered reduction.[26] The less negative $E_{1/2}$ values (−1.18 and −1.84 V) for the reduction of **4** compared to **3g** are consistent with an increased ease of reduction of ligand of **2** as a consequence of its better π-accepting characteristics, as the result of an increase in its extended π-conjugation. Studies of the oxidation waves for **3g** show the presence of quasi-reversible or irreversible oxidation couples at +0.34 and +0.94 V (versus Ag/ Ag$^+$). The first positive oxidation wave is assigned to the Ag(II)/Ag(I) couple. The second positive oxidation wave corresponds to successive oxidation leading to a Ag(III) species formed by a subsequent chemical reaction at the electrode. The presence of both two oxidative and one reductive waves of silver ion suggests that the silver ion present in **3g** and **4** is in the Ag(I) oxidation state.

Conclusion

In summary, the self-assembly of silver ions with two highly conjugated Schiff bases leads to the formation of one coordination network and one discrete rectangular compound. The spacers in the conjugated Schiff-base ligands and the π−π interactions are important determinants of the architectures of the final products. Interestingly, the 1D zigzag Ag(I)-containing coordination polymer **3** is not stable in solution. The degradation of **3** and subsequent reorganization occurs to form a [2 × 2] grid architecture. These Ag(I)−Schiff-base compounds **3** and **4** exhibit unusual luminescence at room temperature that is significantly red-shifted compared to other reported Ag(I) polymers, indicating that such electronic excited-state properties could be finely altered by the combination of electron-rich Ag metal centers and highly conjugated Schiff bases.

(26) Bu, X. H.; Liu, H.; Du, M.; Wong, K. M. C.; Yam, V. W. W.; Shionoya, M. *Inorg. Chem.* **2001**, *40*, 4143−4149.
(27) (a) Ciurtin, D. M.; Pschirer, N. G.; Smith, M. D.; Bunz, U. H. F.; zur Loye, H. C. *Chem. Mater.* **2001**, *13*, 2743−2745. (b) Cariati, E.; Bu, X.; Ford, P. C. *Chem. Mater.* **2000**, *12*, 3385−3391. (c) Wurthner, F.; Sautter, A. *Chem. Commun.* **2000**, 445−446.
(28) Armaroli, N. *Chem. Soc. Rev.* **2001**, *30*, 113−124.
(29) Harvey, P. D.; Fortin, D. *Coord. Chem. Rev.* **1998**, *171*, 351−354.
(30) Liu, Q. X.; Xu, F. B.; Li, Q. S.; Zeng, X. S.; Leng, X. B.; Chou, Y. L.; Zhang, Z. Z. *Organometallics* **2003**, *22*, 309−314.

Experimental Section

Chemicals. Reagents were used as received without further purification. Acetonitrile and nitrobenzene were dried over CaH_2 and were freshly distilled before use. Tetrabutylammonium perchlorate (TBAP) was dried at 100 °C for 24 h prior to use.

Instrumentation. NMR spectra were recorded on a Bruker AMX-400 FT-NMR spectrometer. Elemental analyses were performed by use of a Perkin-Elmer 2400 CHN elemental analyzer. The electronic absorption spectra were recorded on a Hewlett-Packard-8453 spectrophotometer. The emission spectra were measured in deoxygenated CH_3CN solution at ambient temperature with a Hitachi F-4500 fluorescence spectrophotometer. For emission lifetime measurements, a time-correlated single photon counting FL 920 nanosecond spectrometer (Edinburgh instrument) was used. Electrochemical measurements were recorded on a BAS 100B/W EC workstation. The electrochemical cell consisted of a three-electrode configuration (glassy-carbon electrode, platinum counter electrode, $Ag/AgNO_3$ reference electrode). The ferrocene/ferrocenium couple served as an internal reference. The scan rate was 100 mV/s, unless otherwise noted. The cyclic voltammograms were obtained in N_2-saturated CH_3CN with the complexes under investigations (1.0×10^{-3} M) and 0.1 M TBAP as supporting electrolyte with a scanning potential range of $+2.00$ to -2.00 V.

Preparation of N,N'-Bis(pyridin-2-ylmethylene)benzene-1,4-diamine (1). Ligand **1** was synthesized (70%) by usual Schiff-base condensation of 1,4-diaminobenzene and 2-pyridinecarboxaldehyde as reported methods.[31]

Preparation of 3,3′-Dimethyl-N,N'-bis(pyridin-2-ylmethylene)biphenyl-4,4′-diamine (2). Ligand **2** was synthesized by Schiff-base condensation of 3,3′-dimethylbenzidine (1.087 g, 5.12 mmol) and 2-pyridinecarboxaldehyde (1.102 g, 10.30 mmol) and obtained as dark yellow crystals (1.187 g, 3.04 mmol, 59%). ^{1}H NMR (400 MHz, DMSO-d_6): δ 8.72 (ddd, $J = 4.8, 1.7, 1.0$ Hz, 2H, pyridyl H^6), 8.54 (s, 2H, CH=N), 8.20 (dt, $J = 7.9, 0.9$ Hz, 2H, pyridyl H^3), 7.97 (td, $J = 7.3, 1.6$ Hz, 2H, pyridyl H^4), 7.63 (d, $J = 1.5$ Hz, 2H, phenyl H^3), 7.57 (dd, $J = 8.0, 1.9$ Hz, 2H, phenyl H^5), 7.53 (m, 2H, pyridyl H^5), 7.23 (d, $J = 8.2$ Hz, 2H, phenyl H^6), 2.40 ppm (s, 6H, methyl). Anal. Calcd for $C_{26}H_{22}N_4$: C, 79.97; H, 5.68; N, 14.35. Found: C, 79.83; H, 5.82; N, 14.38.

Preparation of $[Ag_2(C_{18}H_{14}N_4)_2(ClO_4)_2 \cdot CH_3CN]_n$ (3). A CH_3-CN solution (7 mL) of $AgClO_4$ (41.4 mg, 0.20 mmol) was carefully layered on the top of a THF solution (9 mL) of N,N'-bis(pyridin-2-ylmethylene)benzene-1,4-diamine (57.2 mg, 0.20 mmol). (*Caution! $AgClO_4$ is potentially explosive and should be handled with care.*) Needlelike yellow crystals of $[Ag_2(C_{18}H_{14}N_4)_2(ClO_4)_2 \cdot CH_3$-CN]$_n$ (**3**) began to form over a few days. One of these crystals was used for X-ray crystallography. The crystals were collected by filtration, washed with ether and CH_3CN, and then air-dried. Yield: 86.4 mg (84%). Anal. Calcd for $C_{38}H_{31}Ag_2Cl_2N_9O_8$: C, 44.38; H, 3.04; N, 12.26. Found: C, 44.10; H, 3.55; N, 12.16. When **3** dissolved in solution, it was transformed into **3g**. ^{1}H NMR (400 MHz, DMSO-d_6): δ 8.89 (d, $J = 7.2$ Hz, 2H, pyridyl H^6), 8.87 (s, 2H, CH=N), 8.17 (td, $J = 7.7, 1.6$ Hz, 2H, pyridyl H^4), 8.10 (d, $J = 7.6$ Hz, 2H, pyridyl H^3), 7.75 (m, 2H, pyridyl H^5), 7.37 ppm (s, 4H, phenyl). FAB-MS: m/z 1875.7, $[\{Ag_4(\mathbf{1})_4\}(ClO_4)_3]^+$.

Preparation of $[Ag_2(C_{26}H_{22}N_4)_2(ClO_4)_2]$ (4). A MeOH solution (5 mL) of $AgClO_4$ (82.9 mg, 0.40 mmol) was carefully layered on a mixture of toluene and nitrobenzene (9 mL) of 3,3′-dimethyl-N,N'-bis(pyridin-2-ylmethylene)biphenyl- 4,4′-diamine (39.0 mg, 0.10 mmol). Platelike orange crystals began to form over a few

days. The crystals were collected by filtration, washed with ether and CH_3CN, and then air-dried. Yield: 25.5 mg (21%). ^{1}H NMR (400 MHz, DMSO-d_6): δ 9.02 (d, $J = 4.5$ Hz, 2H, pyridyl H^6), 8.75 (s, 2H, CH=N), 8.24 (td, $J = 7.7, 1.2$ Hz, 2H, pyridyl H^4), 8.12 (d, $J = 7.6$ Hz, 2H, pyridyl H^3), 7.87 (m, 2H, pyridyl H^5), 7.41 (dd, $J = 8.1, 1.1$ Hz, 2H, phenyl H^5), 7.10 (s, 2H, phenyl H^3), 7.08 (d, $J = 8.4$ Hz, 2H, phenyl H^6), 2.17 ppm (s, 6H, methyl). FAB-MS: m/z 1096.9, $[\{Ag_2(\mathbf{2})_2\}(ClO_4)]^+$. Anal. Calcd for $C_{52}H_{44}$-$Ag_2Cl_2N_8O_8$: C, 52.24; H, 3.71; N, 9.37. Found: C, 52.78; H, 3.57; N, 9.01.

Single-Crystal X-ray Studies. Suitable single crystals of **3** and **4** were selected for indexing and the collection of intensity data. Measurements were performed using graphite-monochromatized Mo Kα radiation ($\lambda = 0.710\,73$ Å) on a Kappa CCD diffractometer for **3** and on a Bruker SMART CCD diffractometer for **4**. Intensity data for **3** and **4** were collected at 298 K and 273(2) K, respectively. For **3**, an empirical absorption correction based on a multiscan method was applied. The structures of **3** and **4** were solved by direct methods and refined by the full-matrix least-squares method on F^2 using the SHELX-97[32] and WINGX[33] program packages, respectively. Basic information pertaining to crystal parameters and structure refinements for **3** and **4** are summarized in Table 1, and selected bond distances and angles are provided in Table 2.

Compound **3** crystallizes in the monoclinic system with space group $C2/c$. Intensity data were collected within the limits $1.958°$ $< \theta < 25.028°$. The asymmetric units contain one Ag atoms, one ClO_4^-, and one ligand **1**. One CH_3CN molecule is situated on crystallographic 2-fold axis, and therefore, only half of the CH_3-CN molecule is present in the asymmetric units. No parameter restraints were applied. Anisotropical thermal factors were assigned to the non-hydrogen atoms. The positions of the hydrogen atoms were generated geometrically, assigned isotropic thermal parameters. The maximum and the minimum peaks in final difference maps were 0.582 and -0.520 e Å^{-3}, respectively.

Compound **4** also crystallizes in the monoclinic system with space group $C2/c$. Intensity data were collected within the limits $1.43° < \theta < 25.06°$. The asymmetric unit contains two Ag atoms, one ClO_4^-, a half ClO_4^-, and two ligand **2**. The half ClO_4^- exhibits a 2-fold axis along the O5$-$Cl2$-$O7 direction in which the oxygen atoms are disordered over six positions where O5 and O7 occupy special positions, at a 2-fold axis, with a site occupation factor (SOF) of 0.5, and other oxygen atoms (O6 and O8) are located in general positions with SOF = 0.75. According to the related stoichiometry of Ag ions and ClO_4^- ions in the asymmetric unit, and in view of the charge balance, a hydroxyl anion with an occupancy of 0.5 must be present in this compound that was assigned as O9. Several solvent molecules were found to be disordered. One water molecule (O10) at a general position and 0.25 H_2O (O11) at a 2-fold axis are present in **4**. In addition, a region of disordered solvent close to the hydroxy anion (O9) is also present in the crystal, which modeled as 0.5 CH_3OH, disordered about a 2-fold axis (C501 is situated special position); therefore, only 0.25 CH_3OH is present in the asymmetric unit. Anisotropical thermal factors were assigned to most of the nondisordered non-hydrogen atoms except those showing severe disorder as explained above. The positions of the C$-$H hydrogen atoms were generated geometrically, assigned isotropic thermal parameters. The hydrogen atoms on solvents (H_2O and CH_3OH) and hydroxyl anion are not located. The maximum and the minimum peaks in the final difference maps were 1.173 and -0.443 e Å^{-3}, respectively.

(31) Shavaleev, N. M.; Bell, Z. R.; Accorsi, G.; Ward, M. D. *Inorg. Chim. Acta* **2003**, *351*, 159$-$166.

(32) Sheldrick, G. M. *SHELX-97* (including SHELXS and SHELXL); University of Gottingen: Gottingen, Germany, 1997.

(33) Farrugia, L. J. *J. Appl. Crystallogr.* **1999**, *32*, 837$-$838.

Supporting Information Available: Crystallographic details, redox potentials, solid-state emission spectra of **3** and **4**, and emission decay profiles of **3g** and **4**. This material is available free of charge via the Internet at http://pubs.acs.org.

IC051235K